ADVANCED FUNCTIONAL MATERIALS
www.afm-journal.de

Fully Bio-Based Epoxy Resins from Liquefied Wood for Chemically Recyclable Wood Coatings

*Qisong Hu, Ricardo P. Martinho, Suna Azhdari, Jean-Paul Lange, Martin van Drongelen, M. Pilar Ruiz, and Frederik R. Wurm**

Epoxy resins are widely used in the coatings industry, yet their petroleum-based origin and crosslinked structures pose challenges for sustainability and recyclability. This study explores a cradle-to-cradle approach for bio-based epoxy wood coatings using the heavy fraction of liquefied wood (LW) as a renewable curing agent. LW, a lignin-like compound rich in aromatic structures, acts as a hydroxyl donor and reacts with biobased glycerol diglycidyl ether (GDE). This article presents the molecular characterization of LW by different techniques. It demonstrates that the resulting coating has a performance comparable to commercial bisphenol A epoxy-amine systems, and shows that the crosslinked product of LW and GDE can be depolymerized and recycled as aromatic polyol using the same liquefaction process. Importantly, this work highlights that the recycling process does not require removing the coating from the wood matrix. Instead, the coated wood, including both the wood and coating, can be recycled together through the same liquefaction process used to produce the LW. This LW-epoxy platform demonstrates the feasibility of creating wood coatings with improved recyclability, contributing to more sustainable practices in the coatings industry.

1. Introduction

Addressing the need for environmentally friendly wood coatings, a recyclable and bio-based epoxy resin has been derived from wood liquefaction and offering properties comparable to commercial coatings.

Coatings are an integral part of modern society, providing protection to various substrates across multiple industries, including electronics, marine, aerospace, automotive, and construction. Among various coatings, epoxy resin coatings are particularly valued for their outstanding durability, mechanical properties, chemical resistance, and strong adhesion.[1] However, the majority of epoxy resins are manufactured from bisphenol A, a petroleum-based compound identified as an endocrine disruptor, raising significant environmental and health concerns.[2,3] Additionally, commonly used hardeners or curing agents, which are able to harden epoxy resins by reacting with them to form a rigid crosslinked network, such as amines, anhydrides, and thiols, are also mostly derived from fossil sources. And the crosslinked nature of traditional epoxy resins further complicates recycling, as the rigid network structure makes it difficult to break down, and the coating itself is hard to detach from the substrate. These factors contribute to increased waste and sustainability challenges. Therefore, there is a need for the development of 2-component epoxy resin systems that are

Q. Hu, S. Azhdari, F. R. Wurm
Sustainable Polymer Chemistry
Department of Molecules and Materials
MESA+ Institute for Nanotechnology
Faculty of Science and Technology
University of Twente
P.O. Box 217, Enschede 7500 AE, the Netherlands
E-mail: frederik.wurm@utwente.nl

Q. Hu, J.-P. Lange, M. P. Ruiz
Sustainable Process Technology
Faculty of Science and Technology
University of Twente
Drienerlolaan 5, Enschede 7522 NB, the Netherlands

The ORCID identification number(s) for the author(s) of this article can be found under https://doi.org/10.1002/adfm.202502689

DOI: 10.1002/adfm.202502689

Q. Hu, M. van Drongelen
Production Technology Group
Faculty of Engineering Technology
University of Twente
Enschede 7500AE, the Netherlands

R. P. Martinho
Biomolecular Nanotechnology
Department of Molecules and Materials
MESA+ Institute for Nanotechnology
Faculty of Science and Technology
University of Twente
P.O. Box 217, Enschede 7500 AE, the Netherlands

S. Azhdari
Institute for Physical Chemistry and Center for Soft Nanoscience (SoN)
University of Münster
Corrensstraße 28–30, 48149 Münster, Germany

bio-based, recyclable, and capable of being recycled along with the substrate in an easy and practical way, without the need to detach the coating from the matrix.

Driven by the demand for sustainable materials, research has focused on the synthesis of both bio-based epoxy resins and corresponding hardeners.[4–9] Among various bio-based resins, glycerol diglycidyl ether (GDE) stands out due to its ease of synthesis and cost-effectiveness.[4] Equally important is the selection of suitable hardeners. While bio-based alternatives, including amines, acids, anhydrides, and polyphenols like lignin or tannic acid have been investigated,[3,10] the heavy fraction of liquefied wood (LW) remains an unexplored option with significant potential.

LW, a bio-based polyphenol from wood liquefaction, offers a novel approach to epoxy resin hardening. Since LW consists only of carbon, hydrogen, and oxygen, it does not introduce any new elements into the epoxy resin, and the hydroxyl groups in LW can react with epoxides to form crosslinked epoxies. Since LW originates from wood, when applied as a coating on wood, it can be recycled together with the wood matrix via liquefaction, eliminating the need to remove the coating beforehand. These characteristics, combined with its bio-based origin, makes LW a particularly promising candidate for sustainable epoxy resin formulations.

While one study has explored LW in plastics and composites,[11] its potential in epoxy resins remains untapped. Current research primarily focuses on the bio-oil obtained from liquefaction, typically used as a low-value fuel or directly using the bio-oil as a curing agent for epoxy resins,[12,13] but this approach raises concerns about the non-reusability of solvents and the low actual biomass content in the final product. In contrast, LW, the residual fraction after solvent extraction from liquefied wood, offers a unique opportunity to develop sustainable and high-performance epoxy systems, which is explored herein.

Beyond the need for bio-based epoxy systems, the development of recyclable resins is a pressing challenge for the coatings industry. Previous efforts to recycle epoxy resins have focused on introducing reversible or active covalent bonds via chemical modification of epoxides or hardeners. Therefore, the cured modified epoxy resins were chemically recycled through reversible chemistries, such as Diels-Alder, transesterification and disulfide exchange reactions. While elegant, these methods often increase raw material costs,[14,15] or require complex solvents or catalysts, such as supercritical 1-propanol with KOH,[16] subcritical water with phenol and KOH,[17] or $AlCl_3/CH_3COOH$,[18] making them less practical for widespread use. Additionally, coatings are inherently complex systems comprising multiple chemical components and, also are typically applied to the surface of a substrate. This close integration with the underlying material, or matrix, poses significant challenges for recycling. Effective recycling often necessitates the separation of the coating from the substrate and the isolation of its various chemical constituents. However, coatings are designed to adhere strongly to the substrate, forming a durable and interconnected system. This intrinsic characteristic complicates separation processes, making the recycling of coatings not only technically demanding but also less practical. As a result, developing efficient recycling methods for coatings that address these challenges remains a critical priority together with advancing bio-based systems.

This study provides an in-depth molecular characterization of LW from pine wood and demonstrates its use as a curing agent for the bio-based epoxide GDE. This approach not only utilizes a fully bio-based epoxide GDE but also allows the solvent guaiacol used in the liquefaction process to be reused, which should enhance the sustainability of the system. We also investigated the performance of the epoxy resin as wood coatings on pine wood, achieving fully bio-based wood coatings that can be recycled through the same liquefaction process for LW (**Figure 1**). Remarkably, the recycled coating (RC) retained its mechanical properties, making it suitable for direct use in the manufacture of new wood coatings without any loss of performance. This work marks an advancement in developing sustainable and recyclable 2-component epoxy resins for coating applications.

2. Results and Discussion

2.1. Liquefaction of Pine Wood

Liquefaction of pine wood was performed in a pressure reactor at 300 °C at 10 bars for 1 h in a tenfold excess of guaiacol as liquefaction solvent, following a previously described method.[11] Pine wood was chosen as a cheap and affordable starting material, compared to other hard woods like oak, maple. Detailed procedures are provided in the Experimental Section. After the liquefaction process, the solvent guaiacol and the light fraction of liquefied wood were removed by vacuum distillation. The heavy fraction of liquefied wood (LW) was obtained as the residue in the form of a black oil, which solidified at room temperature, with a yield of ≈70 wt.% compared to the initial weight of pine wood.

2.2. Coating Recycling

To prove that the obtained coatings based on LW and GDE can be recycled by liquefaction, the product was ground and mixed with guaiacol following the same liquefaction process as described for the initial pine wood. After the removal of the solvent and light fraction, the remaining black solid was designated as the heavy fraction of recycled wood coating (RC) with a yield of 88 wt.%. Notably, similar to LW, RC was fully soluble in organic solvents, like tetrahydrofuran (THF) and dimethyl sulfoxide (DMSO), indicating that the crosslinked structure of the wood coating was destroyed during the liquefaction process.

2.3. Characterization of Liquefied Products

The heavy fraction obtained from pine wood liquefaction exhibits a highly phenolic structure with furanic components, similar to lignin.[19] GPC analysis in THF indicated a similar molar mass of LW, RC and lignin with apparent M_n-values < 1000 g mol^{-1} and M_w-values between 1000 and 2500 g mol^{-1} (**Figure 2A**). These relatively low molar masses are expected, as during liquefaction, depolymerization of wood occurs. Interestingly, the molar mass of the recycled wood coating, RC, showed the highest apparent molar mass, indicating that after the liquefaction recycling, a certain amount of the epoxide GDE chains remained in the RC. Elemental analysis of LW, RC and lignin showed similar composition regarding the ratio of C:H:O (Figure 2B) of 68:6:26 w/w, corresponding to the general chemical formula $CH_{0.09}O_{0.38}$, which

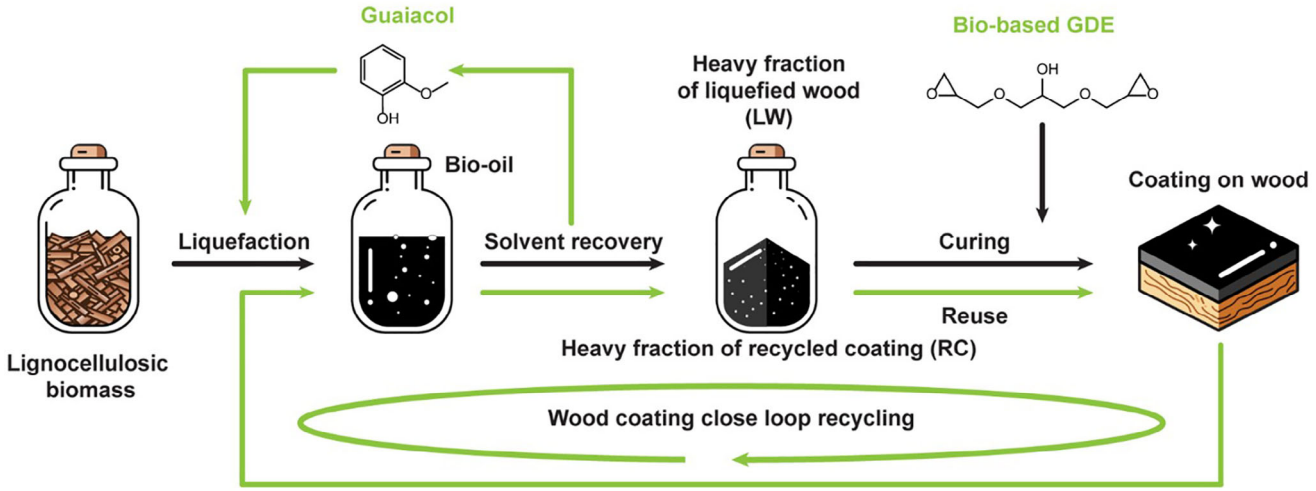

Figure 1. Schematic concept of this study. The heavy fraction of liquefied wood (LW) is produced through the liquefaction of lignocellulosic biomass (pine wood). Wood coatings are synthesized by crosslinking LW with bio-based glycerol diglycidyl ether (GDE) on wood tiles. These wood coatings are subsequently recycled via liquefaction, yielding the heavy fraction of recycled coating (RC), which is reused in the production of new wood coatings.

demonstrated a higher carbon ratio, comparing with guaiacol $CH_{1.14}O_{0.29}$.

To further understand the chemical structure of LW and RC, we used a combination of spectroscopies: FTIR, 1D ^{1}H, ^{13}C, 2D ^{1}H-^{13}C HSQC NMR, and derivatization ^{31}P NMR spectroscopy.

FTIR spectra can provide valuable information on chemical functional groups (Figure 2C). LW, RC, and Kraft lignin exhibit several similar vibrations. For instance, OH stretching can be observed between 3000–3600 cm^{-1}, while CH stretching in aromatic methoxy groups is detected at 2938 cm^{-1}. Additionally, methyl and methylene groups of side chains are present

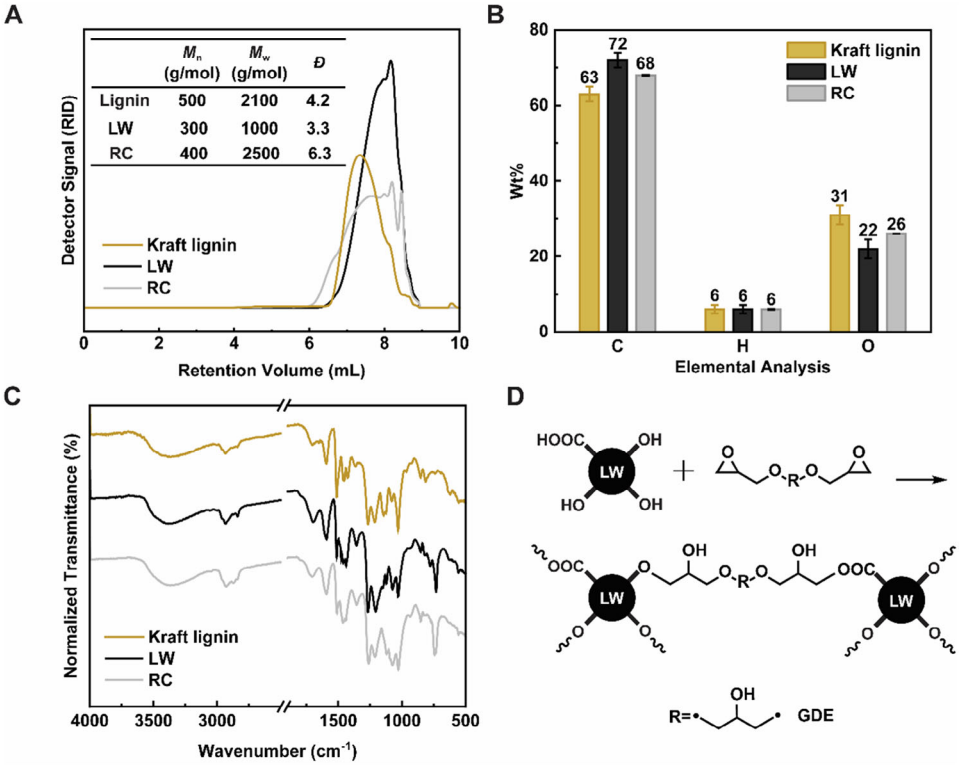

Figure 2. Basic information of LW and RC compared to Kraft lignin (A–C), and the chemical reaction of LW and glycerol diglycidyl ether (GDE) (D). A) GPC elugrams based on refractive index detector using THF as mobile phase; apparent molar masses determined versus polystyrene standards. B) Elemental analysis. C) Overlay of the FTIR spectra of LW, RC and Kraft lignin. D) Crosslinking of LW with epoxide GDE.

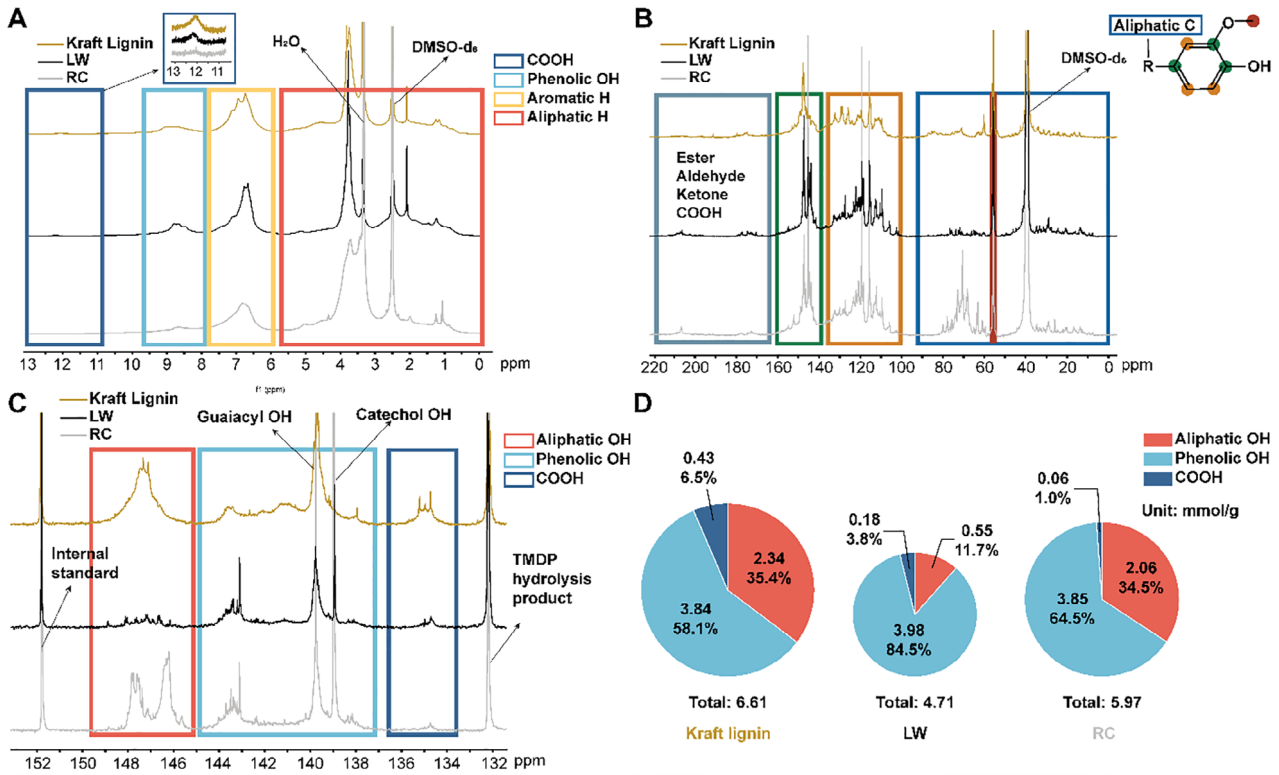

Figure 3. ^{1}H NMR and ^{13}C NMR spectra of LW and RC in comparison with lignin (A,B), and the quantification of OH groups based on ^{31}P NMR spectra (C,D). A) Overlay of the ^{1}H NMR (400 MHz, 298K, DMSO-d_6) spectra of LW, RC and Kraft lignin. B) ^{13}C NMR (600 MHz, 298K, DMSO-d_6) spectra. C) ^{31}P NMR (400 MHz, 298K, Pyridine+$CDCl_3$) spectra of LW, RC and lignin after phosphitylation. D) OH concentration based on ^{31}P NMR spectra. The area of pie chart is proportional to the total OH amount.

at 2842 cm^{-1}, and non-conjugated carbonyl/carboxyl stretching is detected within the range of 1705–1720 cm^{-1}. The spectra also reveal aromatic skeleton vibrations at 1595, 1512, and 1426 cm^{-1}, CH deformation combined with aromatic ring vibration at 1462 cm^{-1}, and aromatic C—H deformation at 1035 cm^{-1}, which is a complex vibration associated with C—O, C—C stretching, and C—OH bending in polysaccharides.[20–23] However, also notable differences exist between LW, RC, and lignin: the absorption at 1654 cm^{-1}, assigned to conjugated carbonyl groups in lignin, is not observed in LW and RC. Furthermore, the signal at 742 cm^{-1}, which likely originates from the guaiacyl-residues attached to the oligomer, where OH correlates with the benzene ring, is absent in lignin because the OH-groups in the guaiacyl monomers in lignin undergoes further linkages with other lignin monomers. As guaiacol is used as a solvent during the liquefaction process, the presence of these peaks suggests that either guaiacol was still present in the samples or was integrated into the LW and RC structures during the liquefaction process. Together with diffusion-ordered ^{1}H NMR spectroscopy (^{1}H DOSY NMR, cf. Figure S4, Supporting Information) we were able to confirm that guaiacol forms covalent bonds with the polymer during the liquefaction (see below). Remarkably, this finding implies that the solvent acts as a reagent, opening the possibility of introducing additional functionalities to heavy fraction of liquefied products depending on the choice of solvent.

^{1}H NMR spectra of LW, RC, and Kraft lignin (**Figure 3A**) exhibited broad resonances in the aromatic (between 7.5 and 6.5 ppm) and aliphatic (between 4.0 and 3.0 ppm for ether-linkages, and between 3.0 and 0.5 ppm for aliphatic resonances) making a detailed structural assignment impossible. However, in DMSO-d_6 as the NMR-solvent, different OH-resonances were detectable: the carboxylic acids were detected between 11.5 and 12.0 ppm, while the phenolic OH groups appeared between 8 and 10 ppm. By adding D_2O to the NMR solution in DMSO-*d6*, these acidic and phenylic OH-protons were deuterated and disappeared from the spectrum (Figure S3, Supporting Information). Generally, LW, RC, and lignin exhibited similar signal patterns, except the carboxylic OH signal is absent in RC.

From the ^{13}C NMR spectra (Figure 3B), Kraft lignin, LW and RC present similar resonances in the aromatic region 100–160 ppm and an intensive peak at 55 ppm, which is contributed to the methoxy group in Ph-OCH_3. However, as both LW and RC did not exhibit any resonances in the 80 to 100 ppm region, we excluded the presence of typical linkages in lignin, such as the β-carbon in the 4-O-β and the α carbon in β-β, β-5 lignin linkages. This strongly indicates that the liquefaction process can cleave the Ar-O-CH-R_2 bonds. In RC, additional resonances between 60–80 ppm indicate the presence of ethers structures from glycerol diglycidyl ether.

A common method in lignin-research to determine the number and type of OH-groups is by phosphitylation, e.g., reaction

with 2-chloro-4,4,5,5-tetramethyl-1,3-2-dioxaphospholane,[24] followed by quantitative ^{31}P NMR analysis (Figure 3C). LW, RC and lignin have a comparable total number of OH groups ranging from 4.7 to 6.6 mmol g^{-1} as summarized in (Figure 3D), while the solvent used for liquefaction, guaiacol, has 8.05 mmol g^{-1}. However, the distributions of OH groups differ significantly: while the content of phenolic OH was similar in all three samples (≈ 3.8 to 4.0 mmol g^{-1}), the content of aliphatic OH was significantly lower in LW than in RC and lignin, accounting for 0.55 mmol g^{-1} versus 2.0 and 2.3 mmol g^{-1}. We assume this is caused by polysaccharides in wood experienced intensively aromatization during the liquefaction, leading to dehydration and loss of aliphatic OH groups. However, the aliphatic OH content in RC increased again due to the introduction of glycerol ethers that apparently are recalcitrant during the liquefaction. Additionally, the COOH content decreased significantly in RC compared to LW, from 0.18 to 0.06 mmol g^{-1}. This can be explained by the reaction of the carboxylic acid groups with GDE and further decarboxylation reactions during the re-liquefaction during recycling. Furthermore, a characteristic resonance for catechol was observed in LW and RC (at 139.0 ppm in Figure 3C), which likely resulted from the reaction and subsequent decomposition of guaiacol during the liquefaction.[25]

Further, the ^{1}H-^{13}C HSQC spectra (**Figure 4A**) supported the finding that liquefaction cleaved the 4-O-β lignin linkage, and β-β, β-5 lignin linkage since they were absent in LW and RC (Green block in Figure 4A).[7,26] The 2D spectra also indicated the presence of keto-containing structures (Hibbert's ketone) at (45.4 ppm, 3.64 ppm) in LW and RC, a structure typically formed during the acidolysis of lignin but absent in Kraft lignin.[27] Furan derivates, commonly obtained from degradation of cellulose or hemicellulose, were also found in LW and RC at (6.06, 106.5 ppm) and (5.90, 107.0 ppm), which correspond to the C3 and C4 positions in the furan structure (Orange block in Figure 4A).[28] Additionally, the resonances at (7.48, 141.0 ppm) were attributed to the C5 position directly connected to the oxygen in furan.[28] These signals were absent in the HSQC spectrum of Kraft lignin. Interestingly, in the HSQC spectrum, resonances that indicate the presence of methylene linkages between two aromatic rings (phenols and/or furans) at (3.88, 29.3 ppm) and (3.83, 34.2 ppm) were detected in LW and RC (Grey block in Figure 4A),[29] which can be rationalized by condensation between different subunits during the liquefaction, similar to a phenomenon observed by Funaoka et al.,[30] who reported that non-condensed units in lignin converted to diphenylmethane-type units upon heating wood meal. This condensation reaction likely also caused the solvent guaiacol to react with LW and RC, leading to an intense FTIR absorption at 738 cm^{-1}. When comparing RC and LW, a significant difference is noted in region between 65 to 75 ppm (in the ^{13}C NMR spectra), which showed resonances originated from the CH_2 groups, attributed to glycerol units in the recycled material (Purple block in Figure 4A). Their presence suggests that liquefaction cannot break all ether linkages between phenol and GDE, resulting in the retention of aliphatic ether groups after recycling. This conclusion was also supported by GPC analysis, which showed an increase in molar mass of RC compared to LW. Also, elemental analysis indicated a slightly increased oxygen and decreased carbon content in RC compared to LW.

Summarizing the analytical data listed above, LW exhibits a similar structure to Kraft lignin, making it a highly phenolic substance. During the liquefaction process, the weaker linkages in lignin, such as 4-O-β, β-5 and β-β bonds, were cleaved. Due to recombination, more stable methylene-linkages were formed. Further, because of the presence of polysaccharides in wood, furan structures were also found after the liquefaction process in LW. In the case of RC, the part of the crosslinking between LW and GDE was broken during re-liquefaction, but some of the glycerol ethers remained within the recycled RC, leading to an increased molar mass and the appearance of additional ether resonances in the NMR spectra. Therefore, in **Figure 5A,B** we propose reasonable/ representative molar structures of LW and RC.

2.4. Curing of LW and RC with Epoxide

For the preparation of wood coatings, LW was cross-linked by reaction with glycerol diglycidyl ether (GDE). We chose the formation of epoxies over other chemistries, as they can be conducted without catalyst and all reagents only contain carbon, hydrogen, and oxygen as elements, making a recycling by re-liquefaction cleaner by avoiding introducing new elements into the system. When LW reacts with epoxides, it forms ether linkages similar to those found in lignin, shown in Figure 2D, which have been shown to be partially cleaved during the liquefaction process. This makes LW-epoxies ideal candidates to create crosslinked materials or coatings that remain chemically recyclable by liquefaction. The molar ratio of the OH-groups in LW to the GDE was varied to determine the optimal formulation and vary the crosslinking density. The samples are coded in the following regarding their formulation, e.g. code "W2G" indicates a twofold excess of OH-groups in LW compared to the epoxide groups in GDE, and the G stands for GDE. "C" stand for the commercial epoxy resin wood coating, which is a bisphenol-A based epoxide-amine system. It was used as a commercial comparison for coating performance.

A 1:1 molar ratio of hydroxyl (OH) to epoxide groups was selected as the starting point to ensure that each reactive site participates fully in the crosslinking process (W1G). This balanced ratio promotes the formation of a well-structured and highly crosslinked polymer network. To investigate the effects of varying the amount of GDE, formulations with different molar ratios of OH from LW to epoxide group from GDE were developed, including W2G (OH groups: epoxide groups = 2:1), W0.5G (OH groups: epoxide groups = 1:2), W0.2G (OH groups: epoxide groups = 1:5). The results showed that when the OH-to-epoxide ratio is too low (excess epoxides, W0.2G), LW and epoxides did not mix well, forming a liquid-paste mixture. Conversely, when the OH-to-epoxide ratio was too high (excess LW), no well-mixed samples were obtained as GDE could not wet the LW powder. For detailed results and observations, refer to Table S1 (Supporting Information).

To understand the kinetics of the curing and the temperatures needed for the later coating process on wood tiles, DSC measurements of the crosslinking polymerization were conducted (Figure S7, Supporting Information). All reactions exhibited an exothermic behavior once the temperature exceeded 100 °C, with exothermic peaks around 150 °C confirming the curing step, i.e.,

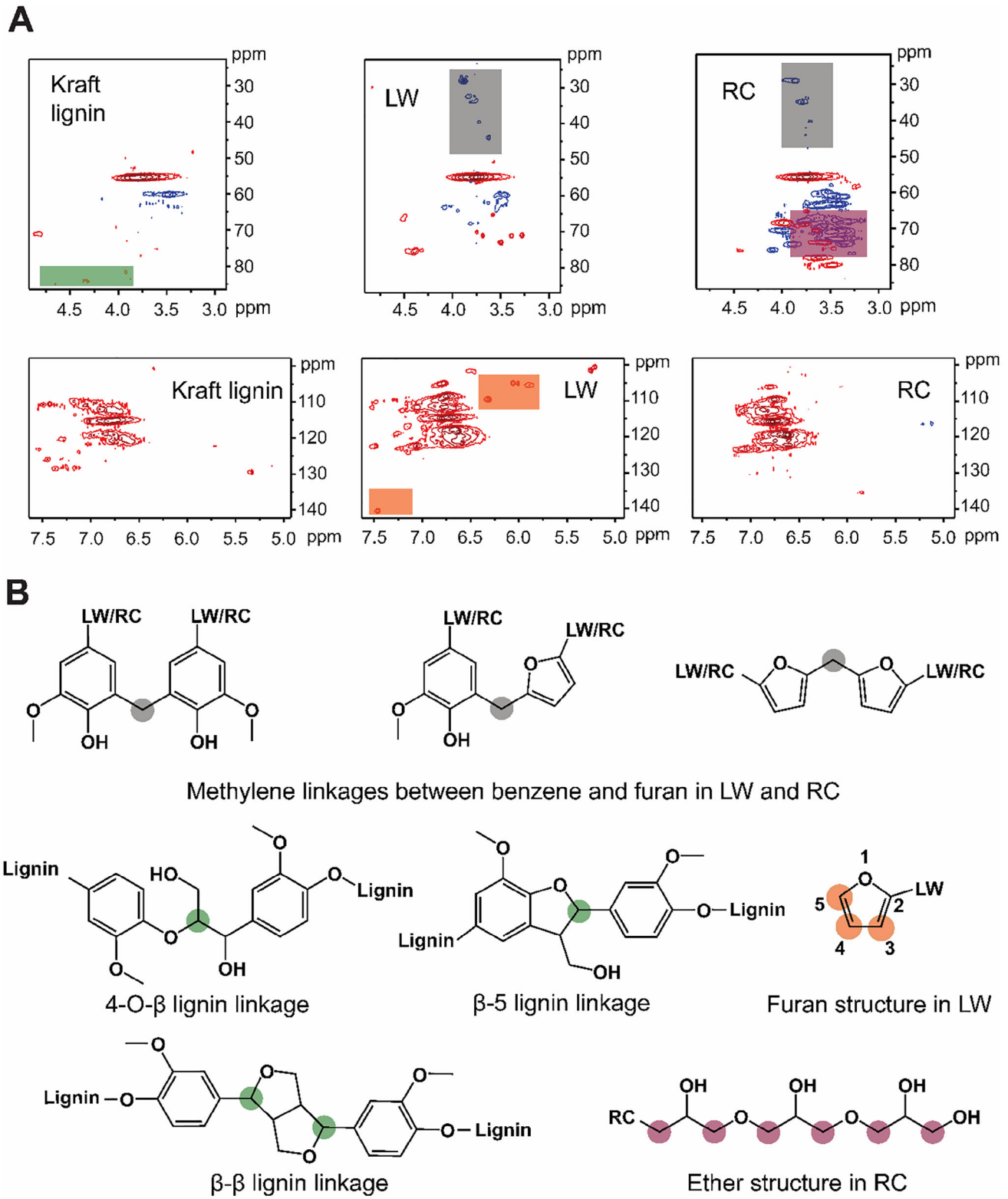

Figure 4. ^{1}H-^{13}C HSQC NMR spectra of LW and RC compared to lignin and proposed chemical structure of LW and RC. A) ^{1}H-^{13}C HSQC NMR (600 MHz, 298K, DMSO-d_6) spectra of LW and RC compared to with lignin. Top: aliphatic region, Bottom: aromatic region. Red: CH_3 or CH, Blue: CH_2. B) Chemical structure found in LW, RC and Kraft lignin, based on ^{1}H-^{13}C HSQC NMR spectra.

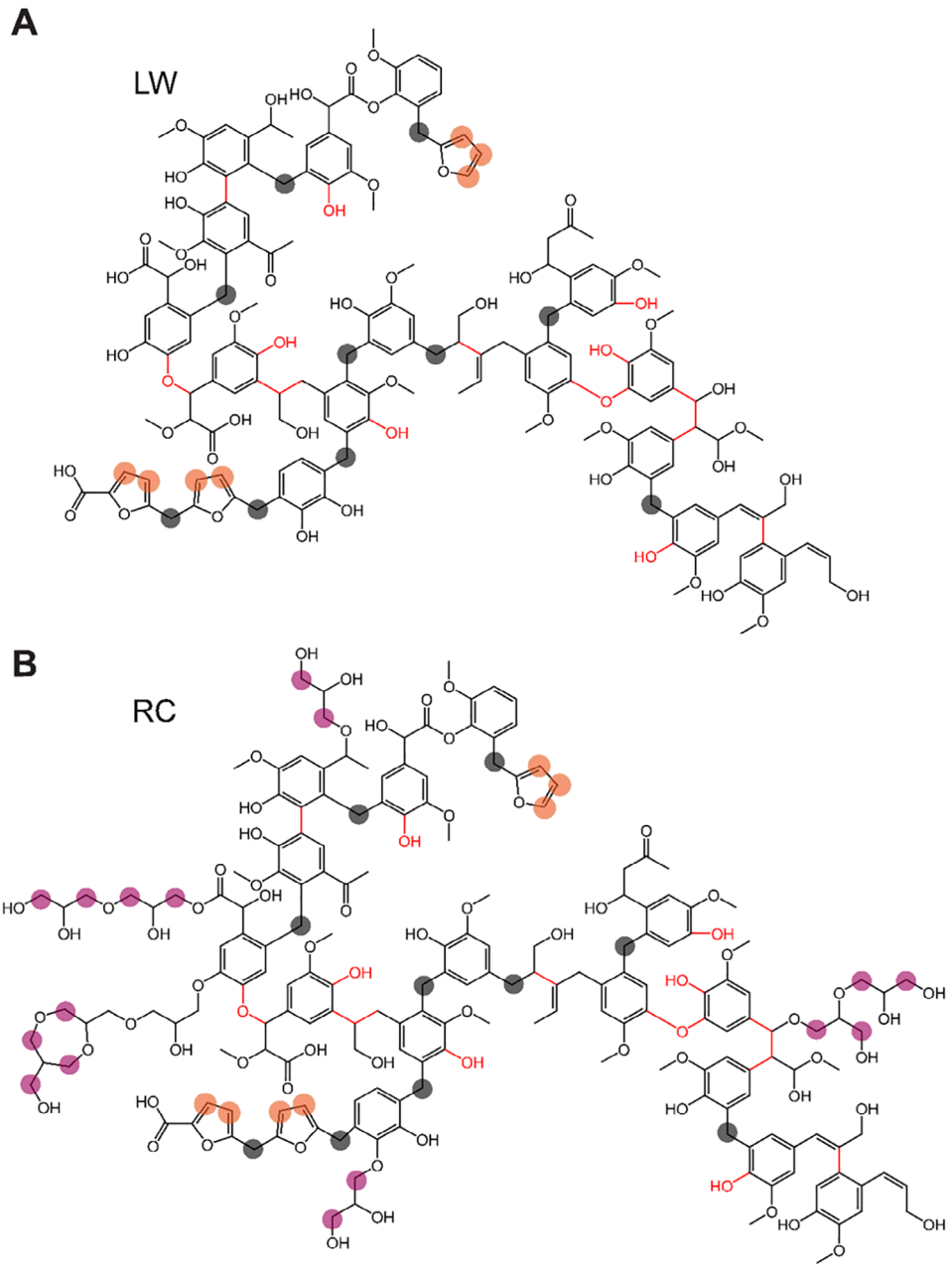

Figure 5. Proposed chemical structures of LW and RC. A) Chemical structure of LW. B) Chemical structure of RC.

the reaction of GDE with LW. Based on the curing-DSC, we chose a temperature of 150 °C for the preparation of the wood coatings. Analysis by FTIR spectroscopy (Figure S8, Supporting Information) further confirmed that the epoxide groups reacted with LW, RC or Kraft lignin completely, since the epoxide-vibration at 910 cm^{-1} vanished after curing (150 °C, 15 h).

2.5. Wood Coatings Manufacture

After understanding the epoxy formulation and curing behavior, pine wood pieces were coated with either LW, or the recycled RC, lignin as a control, and their mixtures with GDE (according to the sample code introduced earlier). To accommodate different test requirements, two sizes of wood coating were produced: 0.1 g of the reaction mixture on 10 × 10 × 4 mm wood tiles and 2.0 g of the mixture on 40 × 40 × 4 mm wood tiles; the samples were cured in oven at 150 °C for 15 h (cf. Experimental Section), resulting ≈ 1.0 mm thick coatings. For the wood coatings on the 10 × 10 × 4 mm wood tiles, intended for nanoindentation tests, the lignin-based formulation (L1G) did not wet the wood surface and failed to form smooth coatings. In contrast, all formulations based on LW and RC produced smooth, glossy, black coatings that – with the naked eye – were indistinguishable from one another.

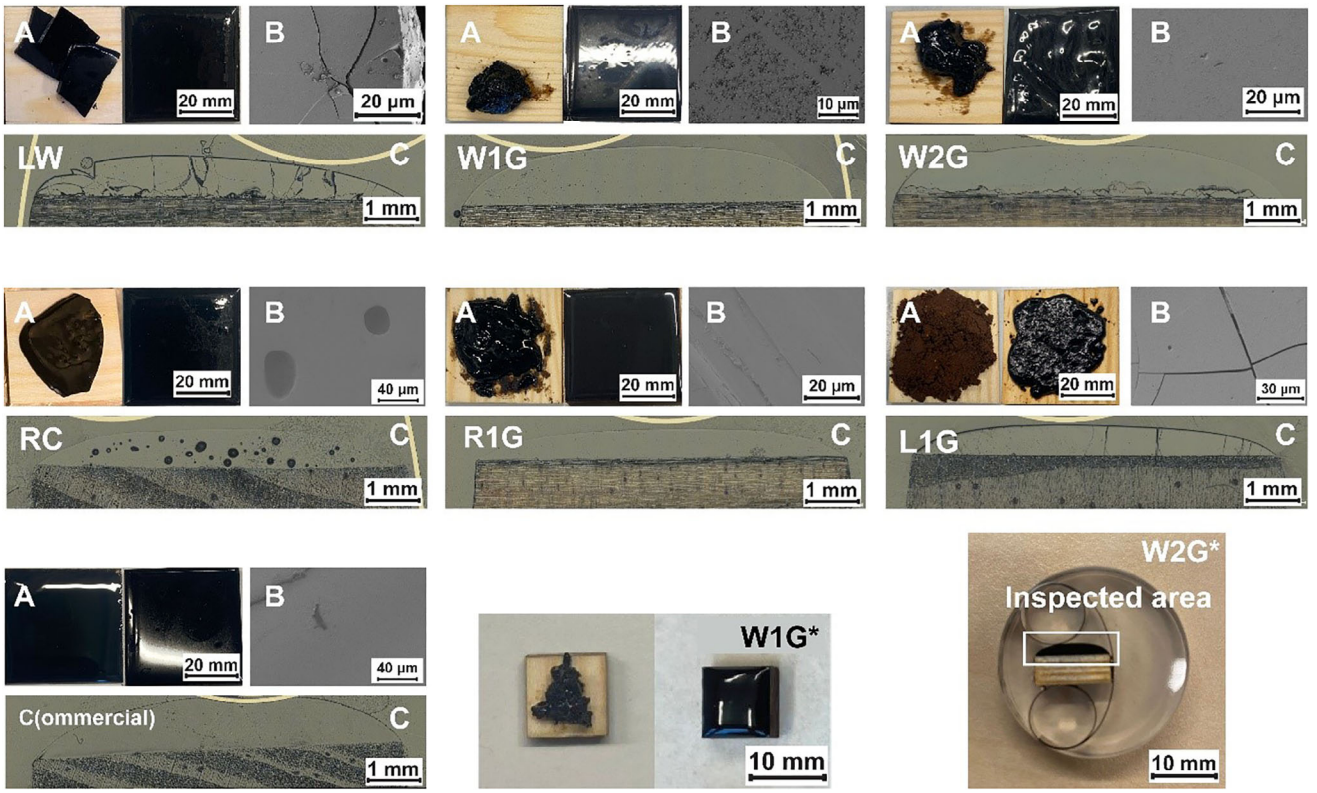

Figure 6. Wood coatings based on LW, RC, or Kraft lignin. A) Photographs of pre- and post-curing coating (on 40 × 40 × 4 mm wood tiles) (left: shows pre-curing; right: shows post-curing at 150 °C for 15 h). B) SEM imagines of cured wood coating (on 10 × 10 × 4 mm wood tiles). C) Light microscopy images of cross section of wood coatings on 10 × 10 × 4 mm wood matrix embedded in epoxy resin. **bottom middle*: a sample of wood coating on 10 × 10 × 4 mm wood substrate is shown; since all wood coatings based on LW, RC are visually identical, only W1G is shown here as a representative example. *bottom right*: photograph of the specimen used for light microscopy.

For the 40 × 40 × 4 mm wood tile, intended for dolly pull-off tests and water contact angle measurements, the reaction mixtures were placed in the center of the wood before curing. During heating, the mixtures liquefied and wetted the wood surface, while simultaneously hardened to form a rigid coating (**Figure 6A**). While most formulations using LW formed glossy, smooth coatings, the sample W2G displayed an uneven, wave-shaped surface. In contrast, L1G, resulted in an irregular and uneven surface as lignin could not wet the surface as no melting occurred. Photographs taken before curing show that the mixtures of epoxides with LW and RC were absorbed into the wood matrix. This soaking likely improved the adhesion of the coating to the wood matrix.

Light microscopy of the cross-section of the coatings (Figure 6C) showed a uniform structure with no phase separation for all polymers in macro-scale. The coatings were subjected to a vertical force due to being fixed by a metal clip, and this force was observed through the deformation of the coatings. This deformation provided a qualitative estimate of toughness. No deformation for W1G, R1G, RC, and C, demonstrating a strong resistance to deformation. However, serious cracks were observed in LW and L1G, which suggested that these samples were relatively brittle. W2G also displayed cracking, but the cracks were confined to the interface between the coating and the wood matrix. Based on the results of light microscopy, the crosslinking with GDE was proved to enhance the toughness of LW.

Light microscopy provides insights into the coatings' phase behavior, but does not reveal any clear micro-phase separation. To further investigate micro-phase separation, we analyzed the cross-sections using scanning electron microscopy (SEM) shown in Figure 6B. The SEM images indicated that, for all samples, no phase separation is visible. However, minor defects in the form of cracks in the coating were observed.

2.6. Crosslinking Efficiency

The gel fraction refers to the insoluble fraction of cured polymers, indicating the extent of crosslinking. THF can dissolve neat LW and RC, making it a suitable solvent to extract non-crosslinked polymer from the coating to determine the sol:gel ratio (**Figure 7A**). Generally, higher gel content implies higher crosslinking density, which promises enhanced mechanical and increased thermal resistance. Among the samples W1G, R1G, and L1G, L1G exhibited the highest gel content, reflecting lignin's higher reactivity toward epoxides due to its significantly higher COOH content. Overall, when the ratio of OH of LW to epoxide groups is less than 1, LW, RC, and lignin can form a highly crosslinked structure with GDE, achieving gel contents above 88 wt.%, which

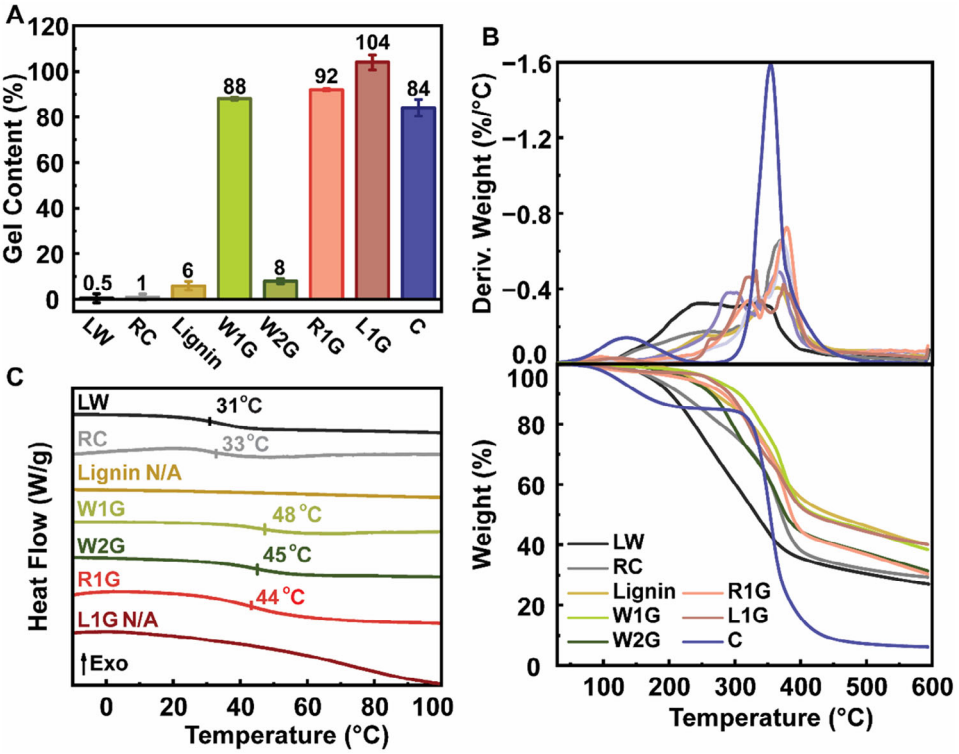

Figure 7. Gel content and thermal properties of cured wood coatings. A) Gel content of wood coating after extraction with THF (after 96 h). B) TGA and DTG of wood coatings, measured at 10 K min^{-1} under nitrogen atmosphere. C) DSC of LW, RC, Kraft lignin and all wood coatings (shown is the 2nd heating at 5 K min^{-1} under nitrogen atmosphere).

is comparable to the commercial epoxy resin (sample C) with 84 wt.%. When the molar ratio of OH in LW to epoxide groups exceeded 1, the gel content remained below 8 wt.%, as seen in samples W2G. This is because the insufficient GDE could not crosslink the LW, resulting in soluble materials.

2.7. Thermal Properties

The thermal stability of all samples was evaluated using thermogravimetric analysis (TGA) (Figure 7B) and expressed as Thermal Heat Resistance Index (T_{HRI}). T_{HRI} of LW increased after curing with GDE, rising from 113 °C (LW) to a maximum of 159 °C (W2G), which is higher than that of cured commercial epoxy resin 123 °C. Additionally, the residue amount of all samples exceeded 22 wt.% at 600 °C, significantly higher than the 6.3 wt.% of commercial epoxy resin, indicating potential benefits for flame retardant applications. The increase in T_{HRI} with more added GDE may be attributed to the cured crosslinked structure and the high boiling point of the GDE. RC exhibited a higher T_{HRI} than LW, similar to that R1G is more thermally stable than W1G. Among all the samples, lignin showed the highest T_{HRI} and residue amount. However, coatings derived from L1G could not form a smooth surface.

DSC was used to study the thermal behavior of cured wood coatings (Figure 7C). Lignin typically has a glass transition temperature (T_g) between 120–180 °C,[31] which may lead to the T_g of L1G was beyond the DSC temperature range limitation of 100 °C (to prevent decomposition inside the machine). In contrast, LW and RC exhibited much lower glass transitions of ≈ 30 °C, probably due to their lower molar mass and different structural elements compared to lignin. After reacting with GDE, the glass transition temperatures of the LW-based coatings were detected in a range from 45 °C to 48 °C. GDE raised the glass transition to 45 °C in W2G, 48 °C in W1G and 55 °C in R1G due to crosslinking. In conclusion, by crosslinking with GDE, the T_g of the LW was improved. Additionally, the presence of only one T_g in the cured wood coatings indicates the absence of phase separation, suggesting a homogeneous structure.

2.8. Surface Water Affinity

Wood coatings are exposed to different humidities depending on their application, making it crucial to understand their water affinity. The water contact angle is an easy method for evaluating the hydrophilicity of coating surfaces (**Figure** 8A). Bare pine wood samples, which have a porous and hydrophilic structure, absorbed water droplets within 20 s. After applying the coatings, water could no longer interface with the wood, making all LW-based coatings suitable as barrier coatings. The non-crosslinked LW exhibited a water contact angle of 62°, which was slightly lower than the water contact angle of the recycled material RC with 72°, indicating that LW has a higher surface hydrophilicity. For GDE-containing coatings increased contact angles of 65° (for W1G) and 85° (for R1G) were measured. Although GDE has

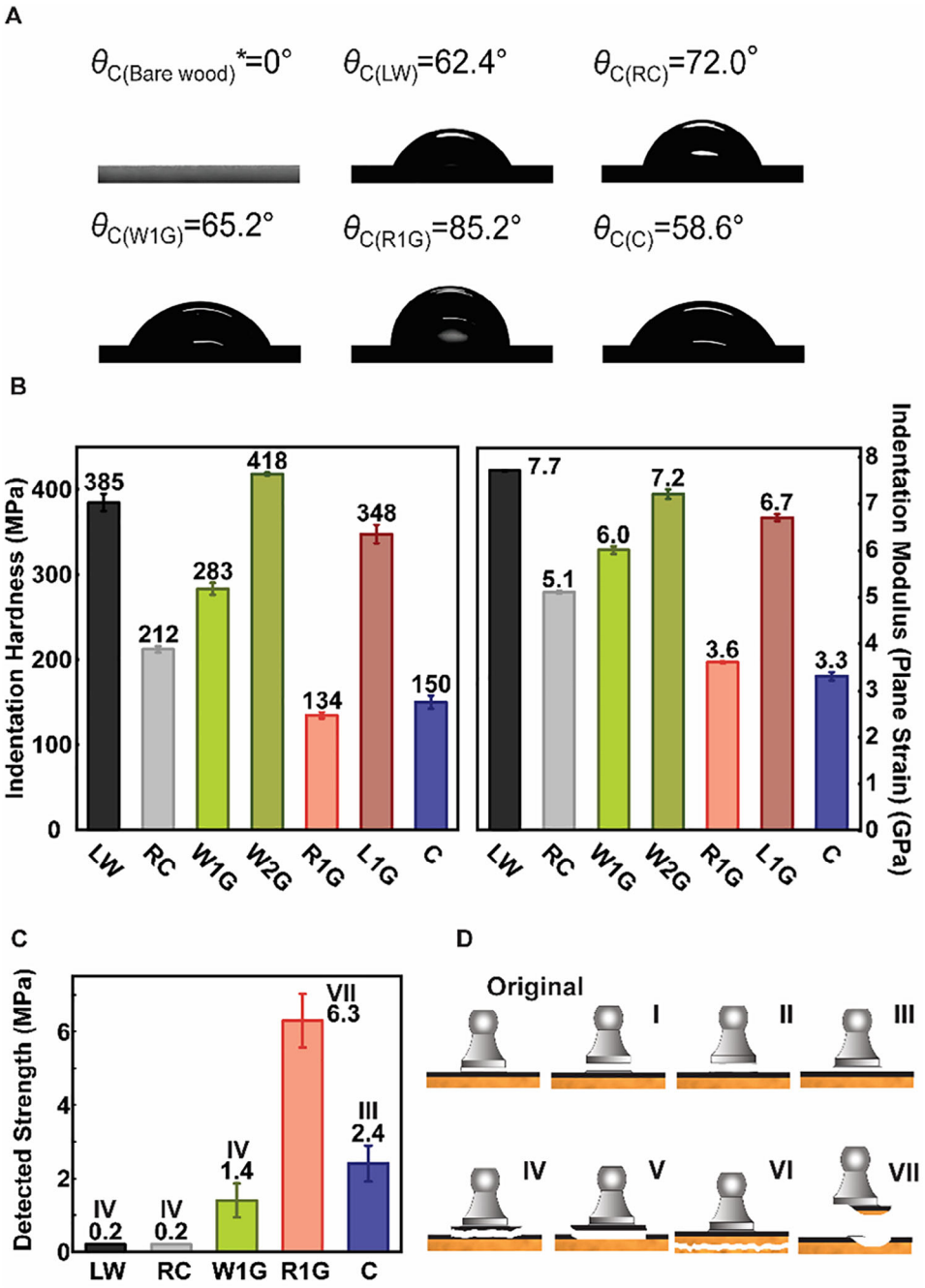

Figure 8. Water affinity and mechanical properties of cured wood coatings. A) Water contact angle of wood coating on 40 × 40 × 4 mm wood substrate after 5 min. B) Nanoindentation test results conducted on the polished surface of cross-section of wood coating. C) Failure model of dolly put off test of coating with the corresponding strength from dolly pull off test. D) Schematic of possible failure models during the dolly pull off test and the interpretations of detected value at break points. I. Break at the interface of dolly and glue: The adhesive strength between dolly and glue; II. Break at the glue layer: The strength of the glue; III. Break at the interface of glue and coating: The adhesion force between glue and coating; IV. Break at the coating layer: The strength of the coating; V. Break at the interface of coating and wood matrix: The adhesive strength between coating and wood matrix; VI. Break at the wood matrix layer: The strength of the wood matrix; VII. Mixed failure: Mixed strength.

hydrophilic glycerol-linkages, its incorporation appears to result in more hydrophobic coatings compared to pure LW and RC. We assume that in the non-crosslinked sample, carboxyl and phenolic groups are present, which readily interact with water, making the surface more hydrophilic and lowering the contact angle. However, during crosslinking, these groups react and form aliphatic hydroxyl groups, which do not ionize in water. This reduces their ability to attract water, making the surface more hydrophobic and increasing the contact angle. Additionally, the commercial epoxy coating showed a contact angle of 59°. This

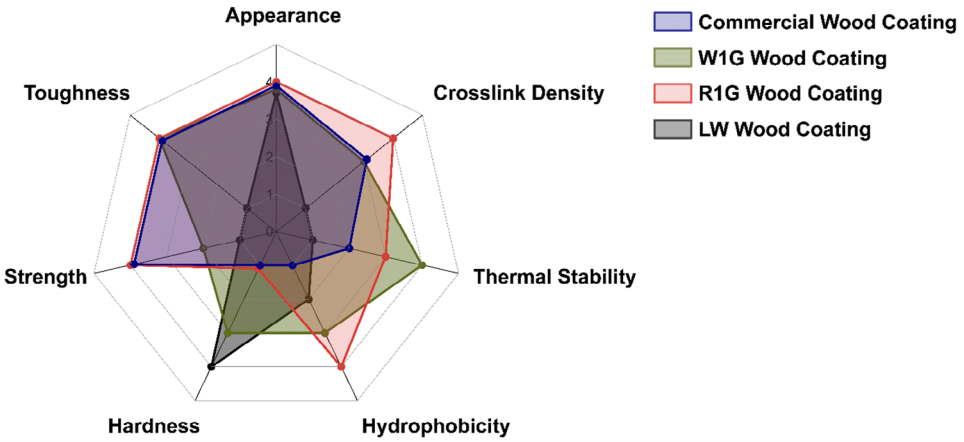

Figure 9. Comparison of Coating Properties. The properties of LW, W1G, R1G wood coatings, and a commercial wood coating reference are compared and ranked from 1 to 4. The rankings are based on appearance (all coatings are identically glossy, smooth by naked eyes, so all are marked as 4), gel content (the most gel content is marked as 4, the least is marked as 1), thermogravimetric analysis (TGA) (the highest T_{HRI} is marked as 4, the lowest is marked as 1), contact angle measurements (the largest contact angle is marked as 4, the smallest is marked as 1), nanoindentation (the hardest is marked as 4, the softest is marked as 1), dolly pull-off tests (the strongest is marked as 4, the weakest is marked as 1. Commercial reference is assumed as 4), and observations under a light microscope (coatings without cracks is marked as 4, with crack is marked as 1).

commercial amine-epoxy resin coating is more hydrophilic compared to LW-based wood coating, probably due the polar amine groups.[32] All other wood coatings exhibited higher surface hydrophobicity compared to the commercial epoxy resin, which is advantageous for waterproofing applications. Due to the uneven surfaces of the W2G, no reliable contact angle measurements could be performed on these samples.

2.9. Mechanical Properties

Hardness is a key factor in evaluating coatings, as it reflects their resistance to abrasion. Nanoindentation is commonly used to measure both hardness and elastic modulus (Figure 8B). LW exhibited an indentation hardness of up to 375 MPa, significantly higher than the 130 MPa of commercial epoxy resin, primarily due to its high aromatic content. In contrast, RC showed reduced hardness due to the introduction of aliphatic ether chains. Surprisingly, crosslinking did not enhance the hardness of the coatings. All wood coatings, except W2G, had lower hardness than LW. The exception in W2G may be attributed to its relatively low GDE content (19%), allowing LW to remain a dominant component and potentially benefiting from crosslinking. Nanoindentation tests were conducted at 1.5 mN, with an indentation depth of 300 nm, suggesting that chemical composition influences hardness more significantly than newly formed crosslinking bonds. L1G showed an indentation hardness of 348 MPa, aligning with lignin's high aromaticity, resulting in greater hardness than RC but lower than LW. The modulus values followed the same trend as hardness.

For coating applications, not only the resistance to abrasion but also the strength of the coating's attachment to the substrate and the strength of coating layer itself are crucial. The dolly pull-off test provides information about the adhesion strength at the interface between the wood coating and the wood matrix and the strength of the coating itself (Figure 8C). However, none of the specimens exhibited the V failure (failure at the support-coating interface), resulting in a lack of accurate data for adhesive strength. Nonetheless, we can still evaluate the range of adhesive strength and the strength or toughness of the coatings. While crosslinking did not significantly alter the hardness, it notably improved the toughness of the coating. Without crosslinking, LW and RC exhibited the IV failure (crack within the coating) and had strengths below the detectable range of 0.2 MPa. After crosslinking, all wood coatings demonstrated increased strength, reaching at least 1.4 MPa (W1G). Interestingly, R1G exhibited a strength of 6.3 MPa at mixed failure (Fail model VII, Figure 8D), suggesting that the actual adhesion or toughness is likely higher than 6.3 MPa. This may be attributed to R1G's high crosslinking level and the presence of moderately soft aliphatic chains, which reduce the hardness and brittleness of the coating, thereby enhancing its toughness. The commercial coating displayed the I failure (failure at the dolly-coating interface), and its measured strength of 2.4 MPa does not provide direct information about the coating itself or its adhesion, making it an unsuitable comparison in this context.

The coating properties of pure LW, W1G, and R1G were summarized (**Figure 9**) and compared to the commercial wood coating. The performance of LW improved significantly when cured with GDE to form the W1G wood coating, with only a slight reduction in hardness. While W1G exhibited slightly lower strength compared to the commercial reference, it demonstrated superior thermal stability, hydrophobicity, and hardness. R1G, derived from the recycling of W1G, showed an overall performance comparable to W1G and, within the investigated performance, even outperformed the commercial wood coating. Most research on bio-based coatings focuses on partially replacing petroleum-based bisphenol A diglycidyl ether or hardeners,[33–36] resulting in coatings that are not fully bio-based. In contrast, W1G is entirely bio-based and recyclable, containing up to 68 wt.% LW and using glycerol diglycidyl ether from renewable sources as its epoxy component. Additionally, LW's softening and

flow behavior at 150 °C eliminates the need for organic solvents, reducing solvent evaporation time, lowering costs, and conserving resources—enhancing overall sustainability. However, further refinements are needed to improve aging resistance, durability, and mitigate the coating's inherent black color. However, further refinement is necessary to address certain limitations, such as improving aging resistance, durability, and overcoming the inherent black color of the coating.

3. Conclusion

This study demonstrated the potential of heavy fractions of liquefied wood (LW) as a sustainable and recyclable aromatic polyol for bio-based epoxy, glycerol diglycidyl ether (GDE). LW, derived from pine wood liquefaction, exhibits a highly phenolic structure similar to lignin, enabling its reaction with epoxides to form durable coatings. However, in contrast to lignin, LW is able to wet the wood substrate effectively, resulting in a homogenous and glossy coating, while lignin only produced brittle unreliable results under these conditions. The resulting coatings from LW, cured with GDE, showed good water resistance and mechanical properties, comparable to commercial epoxy resins. Crucially, these coatings can be chemically recycled through the same liquefaction process used to generate LW, yielding a recycled material (RC) that retains its curing ability and performance. Our approach offers a potential pathway toward environmentally friendly and sustainable epoxy coatings for diverse applications.

4. Experimental Section

Materials: Pine wood (Lignocel 9, Rettenmaier & Söhne GmbH), Kraft lignin (Lineo Classic G by Stora Enso), Guaiacol (≥99%, Sigma Aldrich), Glycerol diglycidyl ether (GDE) (Technical grade, Sigma Aldrich), Dimethyl sulfoxide-d_6 (DMSO-d_6) (99.9 atom % D, Sigma Aldrich), Chloroform-*d* ($CDCl_3$) (99.8 atom % D, Sigma Aldrich), Deuterium oxide (D_2O) (99.9 atom % D, Sigmal Aldrich), *N*-hydroxy-5-norbornene-2,3-dicarboximide (NHND) (97%, Alfa Aesar), 2-chloro-4,4,5,5-tetramethyl-1,3-2-dioxaphospholane (TMDP) (95%, Sigma Aldrich), Chromium(III) acetylacetonate ($Cr(acac)_3$) (97%, Acros Organics), Pyridine (extra dry over molecular sieve, 99.5%, Thermo Scientific), Acetone (>99.5%, Boom), pine wood plank (Schaaflat grenen) were purchased from Praxis as the wood coating matrix, commercial epoxy wood coating (Component A: epoxy resins, including bisphenol A-based and aliphatic glycidyl ethers; Component B: amine-based hardeners, including cycloaliphatic and aromatic amines. Gitzwart- Epoxy Giethars voor oppervlakken) was obtained from Epodex-Nederland. All chemicals were used as received without further purification, except the pine wood was ground and dried in vacuum oven at 45 °C for more than 48 h.

Liquefaction Process to Produce Heavy Fraction of Liquefied Wood (LW): Similar to pervious work,[11] the liquefaction procedure was executed within a 1 L autoclave featuring an electrical heating jacket and agitation. Initially, 75 g dried pine wood and 500 mL guaiacol were introduced into the autoclave. The reactor was then securely sealed and flushed with nitrogen for three times to eliminate any residual air. Subsequently, the N_2 was added again to achieve an internal pressure of 10 bar. The autoclave was then heated to 300 °C, and once this temperature was reached, the reaction was maintained for 1 h. After 1 h, heating was discontinued, and the autoclave was cooled with water until it reached room temperature. The pressure was then released via an outlet valve. The resulting substance was collected and measured, referred to as bio-oil. The solid components were separated from the bio-oil using a 100 mesh iron filter net under 5 bar pressure. Following filtration, the bio-oil was subjected to vacuum evaporation at 3 mbar and 210 °C to remove the guaiacol solvent, continuing the process until all the liquid fraction had evaporated. The residue obtained post-vacuum distillation, with yield of 70 wt.%, was designated as heavy fraction of liquefied wood (LW) and utilized for further investigation.

Recycling of LW-Based Epoxies: The liquefaction of wood coating procedure followed the same protocol as previously described, with the exception of the starting material. Instead of dried pine wood, a cured mixture of LW and GDE in a molar ratio (hydroxyl group from LW to epoxide group from GDE) of 1:1 was used. The resultant product from this process was termed heavy fraction of wood coating (RC) with 88 wt.% yield.

Synthesis of Wood Coatings: Heavy fraction of liquefied wood (LW) and heavy fraction of liquefied coating (RC) were initially ground into a fine powder and subsequently mixed with epoxides. Three types of specimen were produced by heating at 150 °C for 15 h in air environment, and shown in Figure S2 (Supporting Information):

1) 0.5 g sample cured in cylindrical silicone mold with an inner cylinder that has a diameter of 1 cm mould. For FTIR, TGA, gel content and water uptake tests.
2) 0.1 g sample cured on 10 × 10 × 4 mm wood matrix. After the curing, the wood coating was embedded in EpoFix epoxy resin (Struers) and further polished by Struers Tegramin 30 polisher. For light microscope and nanoindentation test.
3) 2.0 g sample cured on 40 × 40 × 4 mm wood matrix. For coating performance test: dolly pull off test and contact angle test.

Supporting Information

Supporting Information is available from the Wiley Online Library or from the author.

Acknowledgements

The authors thank the Dutch Science Foundation (NWO) for funding the project Recyclable Woody Thermoplastic Composites and Coatings (ReWoody), project number (KICH1.ED01.20.002).

Conflict of Interest

The authors declare no conflict of interest.

Data Availability Statement

The data that support the findings of this study are available from the corresponding author upon reasonable request.

Keywords

bio-based coatings, circularity, epoxy resins, liquefaction, wood

Received: January 27, 2025
Revised: March 4, 2025
Published online:

[1] F.-L. Jin, X. Li, S.-J. Park, *J. Indust. Eng. Chem.* **2015**, *29*, 1.
[2] J. Regueiro, A. Breidbach, T. Wenzl, *Rapid Commun. Mass Spectrom.* **2015**, *29*, 1473.
[3] E. A. Baroncini, S. Kumar Yadav, G. R. Palmese, J. F. Stanzione III, *J. Appl. Polym. Sci.* **2016**, *133*, 44103.

[4] R. J. Li, J. Gutierrez, Y. L. Chung, C. W. Frank, S. L. Billington, E. S. Sattely, *Green Chem.* **2018**, *20*, 1459.
[5] C. Zhang, T. F. Garrison, S. A. Madbouly, M. R. Kessler, *Prog. Polym. Sci.* **2017**, *71*, 91.
[6] X. Yang, L. Guo, X. Xu, S. Shang, H. Liu, *Mater. Des.* **2020**, *186*, 108248.
[7] C. Gioia, M. Colonna, A. Tagami, L. Medina, O. Sevastyanova, L. A. Berglund, M. Lawoko, *Biomacromolecules* **2020**, *21*, 1920.
[8] C. Li, J. Dai, X. Liu, Y. Jiang, S. Ma, J. Zhu, *Macromol. Chem. Phys.* **2016**, *217*, 1439.
[9] M. Bučko, K. Kaniaková, H. Hronská, P. Gemeiner, M. Rosenberg, *Int. J. Mol. Sci.* **2023**, *24*, 7334.
[10] Y. Zhang, H. Wang, T. L. Eberhardt, Q. Gu, H. Pan, *Eur. Polym. J.* **2021**, *150*, 110389.
[11] M. P. Ruiz, J. Mijnders, R. Tweehuysen, L. Warnet, M. van Drongelen, S. R. A. Kersten, J. P. Lange, *ChemSusChem* **2019**, *12*, 4395.
[12] M. Kobayashi, Y. Hatano, B. Tomita, *Holzforschung* **2001**, *55*, 667.
[13] M. Kobayashi, K. Tukamoto, B. Tomita, *Holzforschung* **2000**, *54*, 93.
[14] S. Kumar, S. Krishnan, *Chem. Pap.* **2020**, *74*, 3785.
[15] X. Wu, P. Hartmann, D. Berne, M. De bruyn, F. Cuminet, Z. Wang, J. M. Zechner, A. D. Boese, V. Placet, S. Caillol, K. Barta, *Science* **2024**, *384*, adj9989.
[16] H. Yan, C. Lu, D. Jing, C. Chang, N. Liu, X. Hou, *New Carbon Mater.* **2016**, *31*, 46.
[17] Y. Liu, J. Liu, Z. Jiang, T. Tang, *Polym. Degrad. Stab.* **2012**, *97*, 214.
[18] Y. Wang, X. Cui, H. Ge, Y. Yang, Y. Wang, C. Zhang, J. Li, T. Deng, Z. Qin, X. Hou, *ACS Sustain. Chem. Eng.* **2015**, *3*, 3332.
[19] M. C. Barnés, M. M. de Visser, G. van Rossum, S. R. A. Kersten, J. P. Lange, *J. Anal. Appl. Pyrolysis* **2017**, *125*, 136.
[20] T. Rashid, C. F. Kait, T. Murugesan, *Proc. Eng.* **2016**, *148*, 1312.
[21] O. Derkacheva, D. Sukhov, *Macromol. Symp.* **2008**, *265*, 61.
[22] C. G. Boeriu, D. Bravo, R. J. A. Gosselink, J. E. G. Van Dam, *Ind. Crops Prod.* **2004**, *20*, 205.
[23] S. Jia, B. J. Cox, X. Guo, Z. C. Zhang, J. G. Ekerdt, *Indust. Eng. Chem. Res.* **2011**, *50*, 849.
[24] X. Meng, C. Crestini, H. Ben, N. Hao, Y. Pu, A. J. Ragauskas, D. S. Argyropoulos, *Nat. Protoc.* **2019**, *14*, 2627.
[25] Wahyudiono, M. S., M. Goto, *J. Mater. Cycles Waste Manag.* **2011**, *13*, 68.
[26] D. S. Zijlstra, A. de Santi, B. Oldenburger, J. de Vries, K. Barta, P. J. Deuss, *JoVE* **2019**, *143*, 58575.
[27] D. M. Miles-Barrett, A. R. Neal, C. Hand, J. R. D. Montgomery, I. Panovic, O. S. Ojo, C. S. Lancefield, D. B. Cordes, A. M. Z. Slawin, T. Lebl, N. J. Westwood, *Org. Biomol. Chem.* **2016**, *14*, 10023.
[28] S. Constant, C. S. Lancefield, W. Vogelzang, R. K. Pazhavelikkakath Purushothaman, A. E. Frissen, K. Houben, P. de Peinder, M. Baldus, B. M. Weckhuysen, D. S. van Es, P. C. A. Bruijnincx, *Green Chem.* **2024**, *26*, 7739.
[29] X. Zhu, B. Bruijnaers, T. V. Lourençon, M. Balakshin, *Materials* **2022**, *15*, 350.
[30] M. Funaoka, T. Kako, I. Abe, *Wood Sci. Technol.* **1990**, *24*, 277.
[31] Å. Henrik-Klemens, F. Caputo, R. Ghaffari, G. Westman, U. Edlund, L. Olsson, A. Larsson, *Holzforschung* **2024**, *78*, 216.
[32] J. Dong, S. V. Kostjuk, H. Liu, *React. Funct. Polym.* **2023**, *192*, 105726.
[33] X. Wang, W. Leng, R. M. O. Nayanathara, E. B. Caldona, L. Liu, L. Chen, R. C. Advincula, Z. Zhang, X. Zhang, *Int. J. Biol. Macromol.* **2022**, *221*, 268.
[34] D. J. van de Pas, K. M. Torr, *Biomacromolecules* **2017**, *18*, 2640.
[35] J. E. Q. Quinsaat, E. Feghali, D. J. van de Pas, R. Vendamme, K. M. Torr, *Biomacromolecules* **2022**, *23*, 4562.
[36] A. Truncali, T. Laxminarayan, N. Rajagopalan, C. E. Weinell, S. Kiil, M. Johansson, *J. Coat. Technol. Res.* **2024**, *21*, 1875.